Nanoscale

Accepted Manuscript

Cite this: DOI: 10.1039/c0xx00000x

www.rsc.org/xxxxxx

Paper

High Performance Amorphous ZnMgO/Carbon Nanotubes Composite Thin-Film Transistors with Tunable Threshold Voltage

Xingqiang Liu[a], Wei Liu[a], Xiangheng Xiao[a], Chunlan Wang[a], Zhiyong Fan[b], Yongquan Qu[c], Bo Cai[a], Shishang Guo[a], Jinchai Li[a], Changzhong Jiang[a], Xiangfeng Duan[d] Lei Liao[a,*]

Received (in XXX, XXX) Xth XXXXXXXXX 20XX, Accepted Xth XXXXXXXXX 20XX
DOI: 10.1039/b000000x

Abstract: Here we report the fabrication and characterizations of high mobility amorphous ZnMgO/single-wall carbon nanotubes composite thin film transistors (TFTs) with tunable threshold voltage. By properly controlling the ratio of MgO, ZnO and carbon nanotubes, high performance composite TFTs can be obtained with the field-effect mobility up to 135 $cm^2/V \cdot s$, a low threshold voltage of 1 V and a subthreshold swing as small as 200 mV/decade, promising a new solution-processed material for high performance functional circuits. A low voltage inverter is demonstrated with functional frequency exceeding 5 kHz, which is only limited by parasitic capacitance rather than the intrinsic material speed. The overall device performance of the composite TFTs greatly surpasses not only that of the solution-processed TFTs, but also that of the conventional amorphous or polycrystalline silicon TFTs. It therefore has the potential to open up a new avenue to high-performance, solution-processed flexible electronics to significantly impact the existing applications and enable a whole new generation of flexible, wearable, or disposable electronics.

1. Introduction

With exceptional optical transparency, decent mobility and excellent stability, amorphous metal oxide semiconductors have attracted considerable interest as a unique class of materials for thin film transistors (TFTs).[1-2] Among various materials, ZnO,[3-4] ZnMgO (ZMO),[5] In2O3,[6-7] InGaZnO,[8-11] InZnO (IZO),[12] and ZnInSnO,[13-14] have been explored as the promising materials for high device performance. Together with a potentially low-temperature solution processibility, these materials could in principle enable practical and unconventional flexible electronic devices with optical transparency.[15-18] However, the typical mobility of these metal oxide TFTs (1~10 $cm^2/V \cdot s$) is still lower than that of poly-silicon TFTs (10-200 $cm^2/V \cdot s$).[19] The formation of hybrid composite materials could allow for the development of materials with multiple combined advantages over single component building blocks.[20] By incorporating single-wall nanotubes (SWNTs) into the amorphous IZO thin films, we have recently demonstrated that oxide/SWNTs composite TFTs can be created with greatly improved carrier mobility up to 140 $cm^2/V \cdot s$. Additionally, the composite TFTs also showed exceptional mechanical robustness for flexible electronics on plastics.[21] This significant improvements could be attributed to the excellent carrier transport and mechanical flexibility of SWNTs.[22] The improved mobility was attributed to the reduction of the effective channel length by the embedded SWNTs network in the oxide matrix.[23] However, the electrostatic screening effect of the SWNTs in the composite thin film makes the semiconductor oxide between SWNTs difficult to be pinched off, resulting in a depletion mode TFT with a relatively large negative threshold voltage (V_{th}) and large subthreshold swing (*SS*), unsuitable for applications in high-speed low power logic circuits.[24-26] By incorporating high oxygen affinities cations (*e.g.* Mg^{2+}) into oxide matrix, here we report the fabrication of high mobility oxide/SWNTs composite TFTs with tunable V_{th} for low voltage logic application.

It has been shown that V_{th} of oxide thin film transistors can be modulated by the incorporation high oxygen affinities cations into binary and ternary compound metal oxide thin films, such as Mg[27-28] and Ga.[18, 29] Oxygen affinities of these metal ions are higher than that of In, Sn and Zn, resulting in a suppressed carrier concentration to reduce the V_{th}, but also typically coming with a severe mobility degradation.[13,27] Importantly, here we show that high performance TFTs with controllable threshold voltage can be achieved by incorporating SWNTs into an oxide matrix with controlled composition. Amorphous ZMO/SWNTs (a-ZMO/SWNTs) composite TFTs with low V_{th} around 1 V and small SS of 200 mV/decade have been fabricated through a sol-gel route. We further show that these high performance TFTs can

[a]Department of Physics and Key Laboratory of Artificial Micro- and Nano-structures of Ministry of Education, Wuhan University, Wuhan 430072, China.E-mail:liaolei@whu.edu.cn
[b]Department of Electronic & Computer Engineering, Hong Kong University of Science & Technology, Hong Kong SAR, China.
[c]Center for Applied Chemical Research, Frontier Institute of Science and Technology, Xi'an Jiaotong University, Xi'an, 710049, China.
[d]Department of Chemistry and Biochemistry, University of California, Los Angeles, California 90095, United States

be used to create logic inverters with voltage gain and excellent speed performance. Our study defines a clear pathway to high performance amorphous oxide/nanotube TFTs with controllable threshold voltage, and represents a critical step forward in developing high speed oxide TFTs for diverse applications in large area flexible electronics.

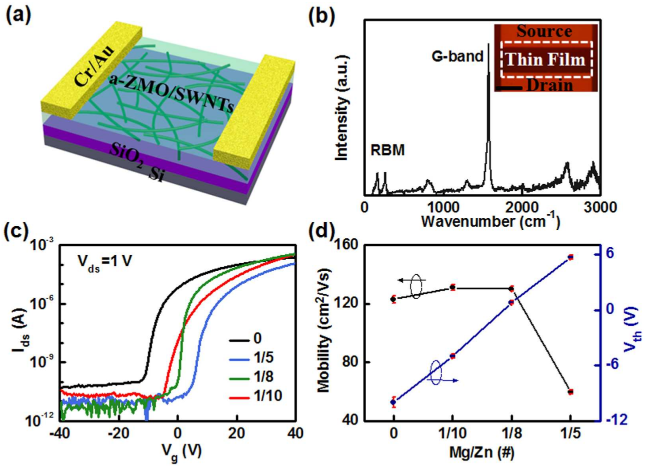

Fig. 1 (a) Schematic of a TFT with the a-ZMO/SWNTs composite active channel. (b) The Raman spectra of the a-ZMO/SWNTs composite thin film in a device channel; the inset shows an optical microscope image of a TFT. The scale bar is 20 µm. (c) The transfer characteristics of the a-ZMO/SWNTs composite TFT with different Mg:Zn molar ratio concentrations. (d) The dependence of mobility and V_{th} on the molar ratio of Mg:Zn.

2. Results and Discussion

2.1. a-ZMO/SWNTs TFTs

A spin-coating process was employed to prepare the a-ZMO/SWCNTs composite thin films on 100 nm SiO_2 coated p^+-Si substrate (Supporting Information S1). Two-step photolithography was employed to fabricate the TFTs. The first photolithography was carried out to define the as-prepared thin film into isolated pads, which can suppress the gate leakage current. The second photolithography was conducted to define source and drain electrodes (S/D). The Cr/Au (15 nm/30 nm) electrodes were completed by metal evaporation and lift-off processes. The transmission electron microscope image of the pure SWNTs used in this work is shown in the Fig. S1. The TFTs geometry employed in this work is shown in Fig. 1a. Fig. 1b is the Raman spectra of the composite thin film in a device channel, which is well consistent with that of SWNTs. The electrical measurements were performed with the Lake Shore TTPX Probe Station and Agilent 4155C Semiconductor Parameter Analyzer. The TFTs with Cr/Au contact are in the linear region operation (V_{ds}=1 V), the transfer characteristics of the fabricated TFTs show typical *n*-type characteristics expected for the oxide matrix (Fig. 1c). The field effect mobility is calculated by using the derivative of transfer characteristics:

$$\mu_{FE} = \frac{g_m L}{V_{ds} C_i W} \qquad (1)$$

where the g_m can be obtained by deriving the I_{ds}-V_g curve. In general, high mobility values exceeding 100 cm^2/V·s are observed in the composite TFTs with relatively low Mg concentration (<10%) (Fig. 1d). It is found that the mobility decreases with the increasing molar ratio of Mg:Zn (*e.g.* 60 cm^2/Vs for Mg:Zn=1:5), which can be attributed to the higher oxygen affinity of Mg than Zn as previously mentioned.[13, 18, 27-29] It is importantly to note that the V_{th} (determined from the horizontal intercept of a linear part in $I_{ds}^{1/2}$ versus V_g plot) can be readily modulated by adjusting the Mg concentration. The TFTs changed from the depletion mode (V_{th}=-11.2 V) to the enhancement mode (V_{th}=6 V) when the Mg:Zn ratio is increased from 0 to 1:5 (averaged over dozens of devices). Together, for composite TFT with a Mg:Zn=1:8, a high mobility value of 130 cm^2/Vs and a small V_{th} of 0.8 V can be simultaneously achieved, promising an attractive TFT material for high performance low power applications. These studies demonstrate the carrier mobility and threshold voltage of composite TFTs can be readily tuned to meet the requirement for specific applications by simply adjusting the molar ratio of Mg in the a-ZMO/SWNTs thin film.

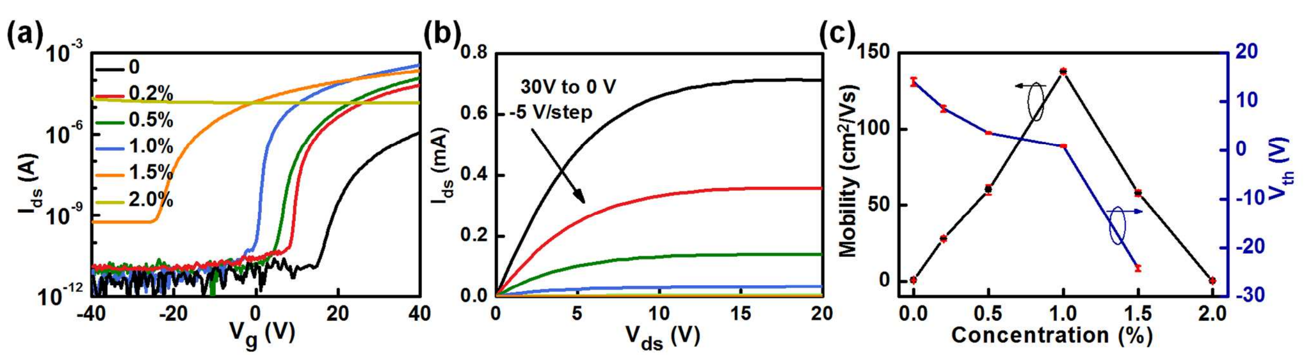

Fig. 2 (a) The transfer characteristics of the a-ZMO/SWNTs composite TFTs with different SWNTs concentrations. The incorporation of SWNTs enhance the mobility, the molar ratio of Mg:Zn is fixed at 1:8. Due to the incorporated SWNTs, the V_{th} shift from the positive towards negative axis. (b) The output character of the composite thin film transistor with 1 wt% SWNTs. (c) The plot of the field effect mobility and threshold voltage as a function of SWNTs concentration.

Dynamic Article Links ►
View Article Online

Cite this: DOI: 10.1039/c0xx00000x

www.rsc.org/xxxxxx

Paper

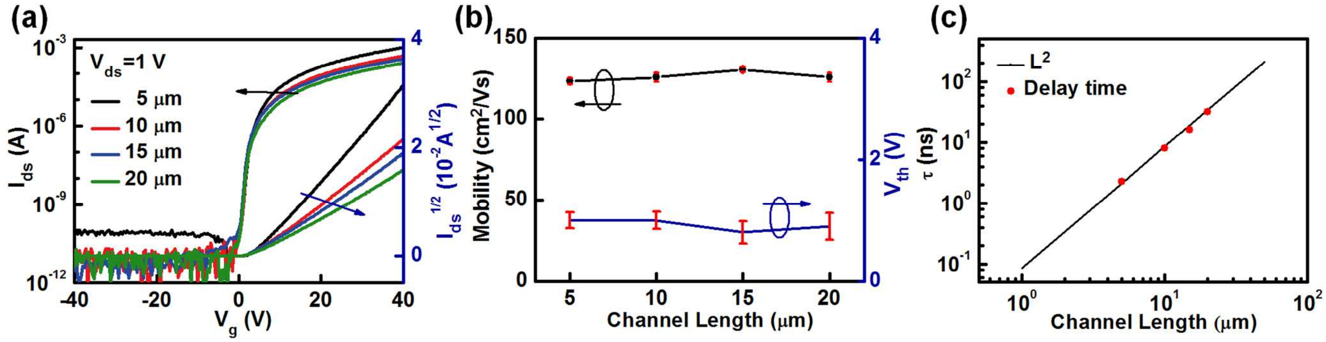

Fig. 3 The performance of a-ZMO/SWNTs composite thin film transistor with different channel length (W is fixed at 75 μm), in which the composite thin film are composed of a-ZMO (Mg:Zn=1:8) and 1 wt% SWNTs. (a) The transfer character curves of the fabricated devices. (b) The plot of mobility and V_{th} versus channel length. (c) Intrinsic delay τ versus channel length. The solid linear is a fit to the data point.

Subsequently, to confirm the 1 wt% SWNTs concentration is also the optimum amount in a-ZMO/SWNTs composite thin film, the TFTs with a fixed 1:8 molar ratio of Mg:Zn with variable SWNTs concentrations from 0 to 2 wt% are fabricated to evaluate the performance of the devices. The transfer characteristics are shown in Fig. 2a. The results are similar to those of the a-IZO/SWNTs composite thin films. Fig. 2b is the output characteristics of the TFT devices with 1 wt% SWNTs. The clear pinch-off and I_{ds} saturation indicate that the carriers transport in active channels is completely controlled by the gate bias.[32] Fig. 2c shows the mobility and V_{th} as a function of SWNTs concentrations, it clearly reveals that the mobility is significantly enhanced as the SWNTs concentration increases in the range of 0-1 wt%. Moreover, the V_{th} drifts to 0.8 V with 1 wt% SWNTs, which is much closer to 0 V. Due to the electrostatic screening effect of SWNTs, high concentration SWNTs weakens the gate field, leading to a degraded mobility and requiring large bias to pinch off the channel, namely, the metallic SWNTs network dominates the carriers transport. These studies demonstrate that 1 wt% SWNTs concentration is also the best recipe for the a-ZMO/SWNT composite thin film.

2.2. a-ZMO/SWNTs TFTs Based Inverter

To probe the reliability and channel length scaling relations of the composite TFTs, we have prepared and studied a-ZMO/SWNT composite TFTs with the channel length L varying from 5 μm to 20 μm. Fig. 3a compares the transfer characteristics of TFTs with different channel length. Fig. 3b summarizes the mobility and V_{th} versus L. The field effect mobility values of the TFTs with different channel lengths are all as large as 130 cm²/V·s. An important benchmark of transistor performance is the intrinsic gate delay time, which represents the fundamental RC (where R is the device resistance and C is the capacitance) delay of the device. It provides a speed limitation for transistor operation, which is relatively insensitive to gate dielectrics and device width. Therefore, the intrinsic gate delay time is used as an important parameter for comparing different types of electronic materials,[33-35] which is given by:

$$\tau = \frac{C_g}{g_m} = \frac{L^2}{\mu_{FE} V_{ds}} \qquad (2)$$

The intrinsic delay time is varied from 2.2 ns for the L=5 μm devices to 31.8 ns for the L=20 μm devices, which is observed at the largest gm. It is also possible to determine intrinsic cut-off frequency equation:

$$f_T = \frac{1}{2\pi\tau} \qquad (3)$$

where the projected f_T of the TFT devices could be up to 72 MHz for the TFT device with a channel length of 5 μm. A summary of τ from a-ZMO/SWNTs composite TFTs versus L is shown in Fig. 4c; the results formations of the devices are fit with L^2. These advantages, together with the low V_{th}=1 V, suggest that a-ZMO/SWNTs composite TFTs can be applied to the fabrication of high-speed inverters with low power-consumption.

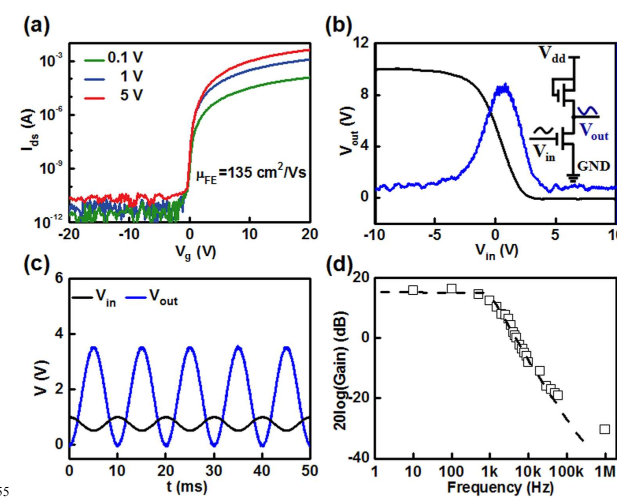

Cite this: DOI: 10.1039/c0xx00000x

www.rsc.org/xxxxxx

Paper

Fig. 4 The DC and AC properties of the inverter. (a) The transfer characteristics of the TFT (with 50-nm SiO_2 insulator) adopted as the 'switch' of the inverter. (b) The voltage transfer characteristic (left vertical axis) and DC gain (right vertical axis) of an inverter, the inverter is schematically depicted in the inset. (c) Output waveform by 0.1 kHz with a sinusoidal signal of V_{pp}=500 mV on the input terminal of the amplifier, (d) AC gain (dB) of the inverter at different frequencies. This inverter shows $f_T > 5$ kHz.

The ability to reliably fabricate high mobility composite TFTs with controllable threshold voltage can readily allow us to construct the functional digital circuits. To this end, we have used two TFTs to configure an inverter. First, high field effect mobility is necessary to achieve large voltage gain inverters.[36-37] Second, a low V_{th}, small *SS* and high *ON/OFF* ratio are necessary to minimize power dissipation.[2, 38-41] Third, a reduced channel length is desirable to minimize the intrinsic gate delay time in high frequency digital circuitry.[42-44] Considering the above requirements, we fabricated a-ZMO/SWNTs TFTs (with 1 wt% SWNTs) on the 50 nm SiO_2 coated p^+-Si, and employed a L/W = 5 µm/75 µm TFTs for the inverter. The transfer characteristic is displayed in Fig. 4a. The field effect mobility is derived from gm with the value as large as 135 cm^2/V·s. Obviously, the SS is decreased to the value of 200 mV/decade. In addition, the a-ZMO/SWNTs TFT is an enhancement-mode device with V_{th}=0.8 V, which is off at V_g=0 V.

To evaluate both the static DC and AC performance of the inverter, we adopt another a-ZMO/SWNTs composite TFT with L/W=500µm/75µm working at the saturation state as the "load". The "switch" TFT with L/W=5µm/75µm is connected with the "load" in series, as shown in the inset of Fig. 4b. The gate of the "switch" TFT acts as the input terminal, whereas the connection between the "switch" and the "load" acts as the output terminal. The static DC performance of an inverter is evaluated by its voltage transfer characteristics and gain shown in Fig. 4b, with V_{dd}=V_{ds}=10 V. The slope of the steepest region of the V_{out}-V_g curve represents the voltage gain G of the amplifier. In this case, the gain of our amplifier is $|G|$=3. It is important to note that a gain higher than 1 is desirable for practical applications. When a small AC signal $V_{in\text{-}AC}$ is superimposed on the DC bias V_g at the input, V_{in}=V_g+$V_{in\text{-}AC}$, then under the right circumstances the transistor circuit can act as a linear amplifier. The transistor is first biased at a certain DC gate voltage to establish a desired current in the circuit. A small sinusoidal AC signal $V_{in\text{-}AC}$ is then superimpose on the gate bias on the input, causing the output voltage V_{out} to oscillate synchronously with a phase difference of 180°, with respect to $V_{in\text{-}AC}$.

For maximum output voltage swing, we supply a gate bias of V_g=1 V to the 'switch' TFT and superimpose small $V_{in\text{-}AC}$ signals of V_{pp}= 500 mV with different frequencies on the gate bias as V_{dd} =V_{ds}=5 V. The amplified output signals with 0.1 Hz is shown in Fig. 4c. For low frequencies (0.1 kHz), the gain $|G|$ defined as$\Delta V_{out}/\Delta V_{in}$ is larger than 6. By measuring the dynamic response of the inverter with a harmonic-waveform input signal from 10 to 1 MHz as shown in Fig. 4d, it is found that the inverter is characterized by a cut-off frequency above 5 kHz. Note that this value is obtained for the TFT with a common gate configuration where a huge parasitic capacitance exists between the Si substrate gate and the large size S/D metal pads. So further performance improvement at the inverter level should also be possible through optimization of the TFT geometry with top-gated structure for small parasitic capacitance.[45]

3. Conclusions

In summary, we have demonstrated high-performance a-ZMO/SWNTs composite TFTs with high field-effect mobility, high ON/OFF ratio and tunable threshold voltage, through the low-cost sol-gel approach. The fabricated a-ZMO/SWNTs TFTs outperform the previous reported amorphous metal oxide based TFTs. Furthermore, the inverter based on a-ZMO/SWNTs TFTs demonstrates high-speed operation. These advantages, together with the demonstrated control over threshold voltage, suggest substantial potential of a-ZMO/SWNTs TFTs for high-performance low cost electronic applications.

4. Acknowledgements

This work is supported by the 973 grant of MOST (No. 2011CB932700), MOE NCET-10-0643 and NSFC grant (No. 11104207, 61222402, 91123009, and 10975109), Hubei Province Natural Science Foundation (2011CDB271), the Natural Science of Jiangsu Grant (BK2011348), the Fundamental Research Funds for the Central Universities under Grant (No.2012202020214 and 2012202020205), as well as " The Grant of State Key Laboratory of Advanced Technology for Materials Synthesis and Processing (Wuhan University of Technology), Early Career Scheme (No. 623112) from Hong Kong Research Grant Council and Special Research Fund Initiative (SRFI) Grants SRF11EG17-B from HKUST. The authors acknowledge helpful discussions with Prof. Zhiyong Zhang at Peking University, Prof. Bozhi Tian at University of Chicago.

Notes and references

1 R. Martins, P. Barquinha, I. Ferreira, L. Pereira, G. Goncalves, E. Fortunato, *J. Appl. Phys.*, 2007, **101**, 044505.
2 N. Dehuff, E. Kettenring, D. Hong, H. Chiang, J. Wager, R. Hoffman, C. H. Park, D. Keszler, *J. Appl. Phys*., 2005, **97**, 064505.
3 R. Theissmann, S. Bubel, M. Sanlialp, C. Busch, G. Schierning, R. Schmechel, *Thin Solid Films,* 2011, **519**, 5623–5628.
4 R. Chen, W. Zhou, M. Zhang, H. S. Kwok, *Thin Solid Films*, 2012, **520**, 6681–6683.
5 W. S. Choi, J. G. Yoon, *Solid State Commun*. 2011, **152**, 345–348.
6 H. S. Kim, P. D. Byrne, A. Facchetti, T. J. Marks, *J. Am. Chem. Soc.*, 2008, **130**, 12580-12581.
7 L. Francioso, M. Russo, A. Taurino, P. Siciliano, *Sens. Actuators. B*, 2006, **119**, 159-166.
8 K. Ebata, S. Tomai, Y. Tsuruma, T. Iitsuka, S. Matsuzaki, K. Yano, *Appl. Phys. Express*, 2012, **5**, 1102.
9 P. Migliorato, M. Seok, J. Jang, *Appl. Phys. Lett.*, 2012, **100**, 073506

10 J. H. Lim, J. H. Shim, J. H. Choi, J. Joo, K. Park, H. Jeon, M. R. Moon, D. Jung, H. Kim, H. J. Lee, *Appl. Phys. Lett.*, 2009, **95**, 012108.

11 M. S. Park, D. H. Lee, E. J. Bae, D. H. Kim, J. G. Kang, D. H. Son, S. O. Ryu, *Mol. Cryst. Liq. Cryst. Sci. Technol.*, 2010, 5**29**, 137-146.

12 D. H. Lee, Y. J. Chang, G. S. Herman, C. H. Chang, *Adv. Mater.*, 2007, **19**, 843-847.

13 M. G. Kim, H. S. Kim, Y. G. Ha, J. He, M. G. Kanatzidis, A. Facchetti, T. J. Marks, *J. Am. Chem. Soc.*, 2010, **132**, 10352–10364.

14 J. Liu, D. B. Buchholz, R. P. H. Chang, A. Facchetti, T. J. Marks, *Adv. Mater.*, 2010, **22**, 2333-2337.

15 M. J. Gadre, T. Alford, *Appl. Phys. Lett.*, 2011, **99**, 051901..

16 J. C. Park, S. Kim, C. Kim, I. Song, Y. Park, U. I. Jung, D. H. Kim, J. S. Lee, *Adv. Mater.*, 2010, **22**, 5512-5516.

17 E. Fortunato, P. Barquinha, R. Martins, *Adv. Mater.*, 2012, **24**, 2945–2986.

18 G. H. Kim, W. H. Jeong, H. J. Kim, *Physica Status Solidi (a)*, 2010, **207**, 1677-1679.

19 K. Nomura, H. Ohta, A. Takagi, T. Kamiya, M. Hirano, H. Hosono, *Nature*, 2004, **432**, 488-492.

20 C. R. Kagan, D. B. Mitzi, C. D. Dimitrakopoulos, *Science*, 1999, **286**, 945.

21 X. Liu, C. Wang, B. Cai, X. Xiao, S. Guo, Z. Fan, J. Li, X. Duan, L. Liao, *Nano. Lett.*, 2012, **12**, 3596-3601.

22 A. Javey, J. Guo, Q. Wang, M. Lundstrom, H. Dai, *Nature*, 2003, **424**, 654-657.

23 S. Kumar, G. Blanchet, M. Hybertsen, J. Y. Murthy, M. A. Alam, *Appl. Phys. Lett.*, 2006, **89**, 143501.

24 N. C. Su, S. J. Wang, C. C. Huang, Y. H. Chen, H. Y. Huang, C. K. Chiang, A. Chin, *IEEE Electron Device Lett.*, 2010, **31**, 680-682.

25 J. Svensson, N. Lindahl, H. Yun, M. Seo, D. Midtvedt, Y. Tarakanov, N. Lindvall, O. Nerushev, J. Kinaret, S. Lee, E. E. B. Campbell, *Nano. Lett.*, 2011, **11**, 3569-3575.

26 C. Avis, Y. G. Kim, J. Jang, J. Mater. Chem. 2012, **22**, 17415-17420.

27 N. Umezawa, M. Sato, K. Shiraishi, *Appl. Phys. Lett.*, 2008, **93**, 223104.

28 H. Wu, J. Liang, G. Jin, Y. Lao, T. Xu, *IEEE Trans. Electron Devices* 2007, **54**, 2856-2859.

29 M. Suh, M. Meyyappan, S. Ju, *Nanotechnol,* 2012, **23**, 305203.

30 J. C. Park, S. W. Kim, C. J. Kim, H. N. Lee, *IEEE Electron Device Lett.*, 2012, **33**, 809-811.

31 J. Y. Choi, S. S. Kim, S. Y. Lee, *Thin Solid Films*, 2011, **520**, 3774–3777.

32 K. Narasimhamurthy, R. Paily, *Semicond. Sci. Technol.*, 2011, **26**, 075002.

33 F. N. Ishikawa, M. Curreli, C. A. Olson, H. I. Liao, R. Sun, R. W. Roberts, R. J. Cote, M. E. Thompson, C. Zhou, *ACS Nano*, 2010, **4**, 6914–6922.

34 J. Y. Kwon, D. J. Lee, K. B. Kim, *Electron. Mater. Lett.*, 2011, **7**, 1-11.

35 J. Xiang, W. Lu, Y. Hu, Y. Wu, H. Yan, C. M. Lieber, *Nature*, 2006, **441**, 489-493.

36 H. Wang, J. Wang, X. Yan, J. Shi, H. Tian, Y. Geng, D. Yan, *Appl. Phys. Lett.*, 2006, **88**, 133508.

37 H. Wang, J. Wang, X. Yan, J. Shi, H. Tian, Y. Geng, D. Yan, *Appl. Phys. Lett.*, 2006, **88**, 133508.

38 K. Banger, Y. Yamashita, K. Mori, R. Peterson, T. Leedham, J. Rickard, H. Sirringhaus, *Nat. Mater.*, 2010, **10**, 45-50.

39 L. Ding, S. Liang, T. Pei, Z. Zhang, S. Wang, W. Zhou, J. Liu, L. M. Peng, *Appl. Phys. Lett.*, 2012, **100**, 263116.

40 M. H. Yoon, H. Yan, A. Facchetti, T. J. Marks, *J. Am. Chem. Soc.*, 2005, **127**, 10388-10395.

41 M. S. Oh, D. Hwang, K. Lee, W. J. Choi, J. H. Kim, S. Im, S. Lee, *J. Appl. Phys.*, 2007, **102**, 076104.

42 T. Sakurai, A. R. Newton, *IEEE J. Solid-State Circuits*, 1990, **25**, 584-594.

43 T. Enoki, K. Arai, Y. Ishii, *IEEE Electron Device Lett.*, 1990, **11**, 502-504.

44 V. Reddy, A. T. Krishnan, A. Marshall, J. Rodriguez, S. Natarajan, T. Rost, S. Krishnan, *Microelectron. Reliab.*, 2005, **45**, 31-38.

45 Z. Liu, H. Li, Z. Qiu, S. L. Zhang, Z. B. Zhang, *Adv. Mater.*, 2012, **24**, 3633–3638

Contents Entry:

High performance a-ZMO/SWNTs composite TFTs with tunable threshold voltage are fabricated by sol-gel method. A low voltage inverter is demonstrated with functional frequency exceeding 5 kHz